

Technical Report

Why is Volumetric Modulated Arc Therapy Not Considered the Standard of Care for Locoregional Radiation Therapy for Breast Cancer Patients?



Robin Kendall, MD, MS,* Tiffany Robinson, BS, Valerie Reed, MD, James Kanke, BS, Alan Sosa, MD, Christopher Nelson, PhD, David Swanson, PhD, Mark Villa, MD, and Elizabeth Bloom, MD

Department of Radiation Physics, Division of Radiation Oncology, The University of Texas MD Anderson Cancer Center, Houston, Texas

Received 10 September 2024; accepted 18 January 2025

We quantify dosimetric differences between 3-dimensional (3D) planning and volumetric modulated arc therapy (VMAT) in breast cancer patients requiring comprehensive regional nodal irradiation (CRNI). Target volume dose, prescription isodose conformity to target volumes, plan hotspots, normal tissue dose-volume metrics, and back and shoulder dose were compared for VMAT and 3D plans of 50 patients. Metrics used to compare VMAT plans with 3D plans included the percentage of primary clinical target volumes (CTVs) receiving 98% of a prescription dose of 5000 cGy, CTV dose hotspots, the extra treatment volume (ETV), and the portion of the patient's body receiving 90% of the CTV prescription dose (excluding the primary target volume). Superior values for these metrics were found for VMAT plans when compared to 3D plans. The mean percentage of the target volume receiving 98% of the prescription dose of 3D plans was 95.4% versus 98.9% among VMAT plans ($P < .01$). The mean target volume hotspot of 3D plans was 7200 cGy versus 5450 cGy for VMAT plans ($P < .01$). A mean ETV found for 3D plans was nearly double that found among VMAT plans (5.3% vs 2.7%, $P < .01$). VMAT plans resulted in lower doses to the shoulder and back. Mean total body volumes of VMAT plans were lower for dose thresholds of 100% to 130% of the prescription. VMAT plans generally had superior values for institutional normal tissue dose constraints. VMAT is superior to 3D planning across multiple metrics for breast cancer patients requiring CRNI. Insurance coverage for VMAT should not require 3D comparison plans.

© 2025 The Author(s). Published by Elsevier Inc. on behalf of American Society for Radiation Oncology. This is an open access article under the CC BY-NC-ND license (<http://creativecommons.org/licenses/by-nc-nd/4.0/>).

Introduction

Volumetric modulated arc therapy (VMAT) offers conformal, normal-tissue-sparing radiation therapy.^{1,2} In certain scenarios, literature exists to support its superiority over 3-dimensional (3D) techniques.³⁻¹⁴ For breast

cancer patients requiring comprehensive regional lymph node irradiation (CRNI), radiation therapy planning is complicated. In addition to the breast or chest wall, axillary, supraclavicular, and internal mammary nodes are treated.¹⁵⁻¹⁸ VMAT and 3D planning are both available at our institution for this. VMAT is often needed in lieu of 3D planning due to several factors that increase lymph node depth, namely, the rising prevalence of obesity in the United States,¹⁹ the increased use of tissue expanders placed post mastectomy^{20,21} (to preserve skin for breast reconstruction, which often requires their expansion during radiation therapy to optimize skin preservation²²⁻²⁴),

Sources of support: This work had no specific funding.

Research data are stored in an institutional repository and will be shared on request to the corresponding author.

*Corresponding author: Robin Kendall, MD, MS; Email: rlkendall@mdanderson.org

<https://doi.org/10.1016/j.adro.2025.101728>

2452-1094/© 2025 The Author(s). Published by Elsevier Inc. on behalf of American Society for Radiation Oncology. This is an open access article under the CC BY-NC-ND license (<http://creativecommons.org/licenses/by-nc-nd/4.0/>).

and/or the presence of an intact breast during radiation therapy. When limited to 3D techniques, target volume dose delivery with adequate normal-tissue-sparing is challenging. Nevertheless, insurance companies require the creation of more rudimentary 3D plans to demonstrate the superiority of a VMAT plan before authorizing use of the latter to avoid its higher reimbursement (policy specifics vary among providers and often deviate from American Society for Radiation Oncology guidelines²⁵). This is unfortunate because VMAT's necessity can usually be ascertained by anatomic inspection, which is poignant because it obviates resources consumed by 3D comparison plan creation. Such policies are onerous and can delay treatment, which is problematic not only for patients, but also for their multidisciplinary care team. Also, it poses a risk for interval disease progression as well as financial toxicity for the patient. In summary, insurance policies requiring the comparison of 3D plans increase health care costs and put treatment success at risk.

In this study of VMAT and 3D radiation therapy for patients requiring CRNI to the breast or chest wall, we provide further evidence supporting a general superiority of VMAT over 3D techniques. We selected patients requiring CRNI for the breast or chest wall treated with VMAT. Comparison 3D plans were created using institutional methods. Metrics to compare techniques included the primary clinical target volume (CTV) percentage receiving 98% of the prescription dose, primary CTV dose maxima ("hotspots"), "excess/extra treatment volume" (ETV), body volumes receiving doses in excess of 100% to 130% of the primary CTV prescription dose, and organ-at-risk (OAR) dose-volume statistics. Additionally, dose statistics of the back and shoulder were compared as their correlation with upper limb function following radiation therapy has been previously established.^{26,27}

Methods and Materials

Treatment plans of 50 breast cancer patients who received CRNI (axillary, supraclavicular, and internal mammary nodal chain) to the chest wall or intact breast with VMAT for unilateral disease between 2020 and 2023 were included (IRB number can be provided on request). All presented with stage II or greater breast cancer with indications for locoregional postoperative radiation including the regional lymph nodes). Cases were selected from only 2 radiation oncologists to minimize interphysician contouring uncertainties. Patient demographics are outlined in Table 1.

Patients were simulated supine while holding onto a T-bar with their arms resting on a "wingboard" (Civco C-Qual breastboard, CQ Medical); arms were in flexion overhead. The wingboard angle was set to avoid breast tissue override of the supraclavicular fossa while minimizing

Table 1 Patient demographics

Patient age: range/median (y)	(30-73)/50
Disease laterality	
Left	23
Right	27
Surgical status	
Intact breast	19
Mastectomy with tissue expander for breast reconstruction	19
Mastectomy without tissue expander	12

inframammary skin folds. For 49 patients, deep-inspiration breath hold was used during planning; 1 patient was planned based on free-breathing anatomy. Open face masks immobilized the head and neck.

CTV contours were per Rad Comp Breast Atlas guidelines²⁸ and received peer review. For chest wall patients, subcutaneous tissue to a depth of 3 mm was not included in the CTV (CTV_{CW}). The CTV of intact breast patients (CTV_{IB}) did not include tissue within 5 mm of the skin. In this study, CTV_{CW} or CTV_{IB} are collectively designated as CTV^{Target}. Lymphatic CTVs included axillary node levels I to III (AX), supraclavicular nodes (SCV), and internal mammary nodes (IMN). CTV_{SCV} did not include any overlap with the esophagus or thyroid. CTV_{AX}, CTV_{SCV}, and CTV_{IMN} did not include any tissue within 3 to 5 mm of the skin surface. All target volumes were contiguous to avoid the creation of local dose minima resulting from gaps between target volumes. The CTV^{Target} to PTV (planning target volume) margin was 5 mm in all directions except inferiorly toward the lung. Here, a 3-mm expansion was used. Chest wall PTVs (PTV_{CW}) did not extend to within 3 mm of the skin surface. Intact breast PTVs (PTV_{IB}) did not extend to within 5 mm of the skin surface. The supraclavicular PTV (PTV_{SCV}) was generated by expanding CTV_{SCV} by 5 mm in all directions except medially toward the trachea, thyroid, and esophagus where no margin was used. A 5-mm isotropic expansion of CTV_{AX} and CTV_{IMN} created axillary (PTV_{AX}) and internal mammary nodal (PTV_{IMN}) PTVs (except any tissue within 3 mm of the skin surface was excluded). To avoid ambiguity, for any volume generated by such expansions in which a higher dose target volume overlapped with a lower dose target volume, the former was subtracted from the latter.

Segmented normal tissues included the ipsilateral and contralateral lung (each with distinct dose-volume constraints as outlined in Table 2), heart, left ventricle, thyroid, spinal cord, ipsilateral brachial plexus, contralateral breast, and esophagus. The stomach and celiac plexus were segmented for patients with left-sided disease—and the liver for patients with right-sided disease. The back and shoulder were segmented based on the anatomic

Table 2 Dosimetric evaluation metrics of treatment planning objectives

Dose evaluation metric	Number	3D mean (SD)	VMAT mean (SD)	P value
Ipsilateral brachial plexus, maximum dose \leq 5200 cGy	50	5411.3 cGy (528.2)	4951.7 cGy (155.6)	<.01
Contralateral breast/chest wall, mean dose \leq 500 cGy	50	157.8 cGy (290.9)	505.0 cGy (160.9)	<.01
Celiac plexus/gastroesophageal junction, maximum dose \leq 1000 cGy	23	85.4 cGy (34.6)	240.5 cGy (63.0)	<.01
Celiac plexus/gastroesophageal junction, mean dose \leq 300 cGy	23	59.5 cGy (26.4)	169.9 cGy (51.7)	<.01
Esophagus, maximum dose \leq 4500 cGy	50	3710.9 cGy (1086.8)	3460.0 cGy (570.7)	.12
Heart mean dose \leq 500.0 cGy	50	387.0 cGy (263.4)	383.6 cGy (65.4)	.92
Heart, $V_{10} \leq 15\%$	50	10.0% (8.4)	2.5% (2.1)	<.01
Heart, $V_{20} \leq 4\%$	50	4.6% (5.4)	0.1% (0.2)	<.01
Left ventricle, $V_5 \leq 25\%$	48	10.2% (14.8)	10.0% (12.6)	.89
Liver, mean dose \leq 1000 cGy	27	269.5 cGy (198.1)	485.8 cGy (165.2)	<.01
Contralateral lung, $V_{20} \leq 8.0\%$	50	0.4% (1.7)	1.2% (1.1)	<.01
Ipsilateral lung, mean dose \leq 2000 cGy	50	2221.4 cGy (263.3)	1567.2 cGy (144.7)	<.01
Ipsilateral lung, $V_{10} \leq 68\%$	50	62.6% (10.1)	52.5% (8.1)	<.01
Ipsilateral lung, $V_{20} \leq 33\%$	50	47.9% (6.9)	28.4% (3.1)	<.01
Spinal cord, maximum dose \leq 2000 cGy	50	2212.1 cGy (1549.8)	1868.6 cGy (140.2)	.13
Stomach, mean dose \leq 500 cGy	23	189.2 cGy (188.0)	284.9 cGy (129.4)	<.01
Thyroid, mean dose \leq 2000 cGy	50	2320.4 cGy (612.6)	1907.2 cGy (255.3)	<.01

Abbreviations: 3D = 3-dimensional; VMAT = volumetric modulated arc therapy.

definitions published by Bazan et al.²⁶ Finally, the patient's scanned total body volume was segmented (represented by V_{TB}). At a minimum, patient computed tomography simulations encompassed a volume extending from the skull base and through the liver.

The CTV_{Target} prescription dose was 5000 cGy. The minimum prescription dose for the axillary, supraclavicular, and internal mammary nodal volumes was 4500 cGy. Multiarc, 6-MV VMAT plans were the baseline for this study. Start and stop angles of each arc were chosen to optimize target volume dose delivery. Plans were designed to fulfill the goal of delivering 95% of each PTVs prescription dose to 95% of its volume. Additionally, plans were optimized so that 98% of the CTV_{Target} prescription dose was delivered to 98% of its volume while also respecting institutional normal tissue treatment planning criteria shown in Table 2.

A 3D plan complimentary to each VMAT plan was designed using institutional 3D planning guidelines. These plans used breast/chest wall tangent fields to treat the CTV_{Target} . Gantry angles were chosen so that, in combination with the jaw and collimator settings, a nondivergent match line was formed on the posterior border. The depth of this match line was chosen so that the target planning structures could be covered while minimizing the dose to the ipsilateral lung and heart. Collimator angles, couch angles, and superior blocks (created with a multileaf collimator) were chosen so that the superior edges of the exposed portion of the opposing tangent

fields were coplanar. Field apertures of the tangential fields were designed to create at least 2 cm of flash from the projection of the skin surface within the field aperture.

Anterior-oblique fields were used to deliver the respective prescription dose to the CTV_{SCV} . The inferior border of the SCV field was designed so that it was also coplanar with the superior borders of the tangent fields. In this manner, a "matched plane" is created between the tangent fields and the SCV field. The lateral edge of the SCV field was blocked so that at least a portion of the humeral head and acromioclavicular joint were shielded from dose delivery. A medial block was created to shield the spinal cord. The superior edge of SCV field extended 5 to 10 mm from CTV_{SCV} to exclude it from beam penumbra and ensure therapeutic dose delivery to CTV_{SCV} . Certain patients with extensive SCV disease required a posterior supplemental field to help improve coverage to the posterior aspect of CTV_{SCV} .

To adequately deliver therapeutic dose to the CTV_{IMN} , some 3D plans employed the well-described use of "wide tangents."²⁹ Other plans followed a commonly used technique employing electron fields to treat CTV_{IMN} .³⁰ Invariably, when photon beams are juxtaposed with electron beams, "cold spots" are present within the electron field while "hotspots" are created within the photon fields. To mitigate and balance cold spots within the CTV_{IMN} and "hotspots" in adjacent target volumes, the line of abutment between photon and electron fields was fine-tuned as needed.

For all plans, the initial photon energy selected in the design process was 6 MV. Attempts were made to achieve the same minimum dose delivery criteria for target volumes that were achieved with VMAT plans. High energy photon beams (15 MV) were employed when necessary to fulfill this portion of the planning objectives. Dose distribution heterogeneity was mitigated with a manual step and shoot technique.³¹ This process involved creating regions of interest (ROIs) from isodose volumes corresponding to doses in excess of various thresholds above the prescription dose. Iteratively, control points employing blocks that obscured these ROIs were created to achieve an acceptable level of dose heterogeneity within target volumes. Although fulfillment of institutional normal tissue dose constraints was attempted, whenever it competed with sufficient target volume dose delivery, this latter objective was favored. When electron fields were used to treat the CTV_{IMN}, an electron beam energy was selected so that the deep surface of the CTV_{IMN} was encompassed by the prescription dose so that the paired VMAT plan's coverage was matched. As previously mentioned, the photon/electron field match line was positioned to achieve a balance in hot and cold spots on each side of the match line.

3D and VMAT plan metrics were selected to quantitatively compare plans on a variety of axes. Dose heterogeneity within the primary CTVs^{Target} as well as within a patient's V_{TB} was assessed. We used the percentage of CTV^{Target} receiving 98% of the prescription dose of 5000 cGy (ie, 4900 cGy), hereafter designated as CTV₄₉₀₀^{Target}, as a measure of sufficient primary target volume dose coverage. The CTV^{Target} dose maximum ("hotspot") was defined as the value on the CTV^{Target} cumulative dose-volume histogram corresponding to an absolute volume of 2 cm³. This metric will be referred to hereafter as CTV_{HS}^{Target}. For a global assessment of dose heterogeneity, the total patient body volumes encompassed by dose thresholds of 100% to 130% of the CTV^{Target} prescription dose were compared (denoted as V₅₀₀₀^{Body}, V₅₂₅₀^{Body}, V₅₅₀₀^{Body}, V₅₇₅₀^{Body}, V₆₀₀₀^{Body}, V₆₂₅₀^{Body}, and V₆₅₀₀^{Body}). These volumes were normalized to V_{TB} and are therefore expressed as a percentage of V_{TB}. These parameters were examined in order to capture and adequately represent plans with volumes receiving particularly high dose values, or overall "hot-spots" which can be seen in 3D plans that employ abutting electron and photon beams and/or in patients with a large tangent field separation.^{32,33}

Additionally, the conformity of a plan's therapeutic isodose surface to the volume of the CTV^{Target} was assessed by calculating an "excess treatment volume" (ETV). The ETV was defined as the volume encompassed by an isodose surface corresponding to a dose equal to 90% of the CTV^{Target} prescription dose, but not including the CTV^{Target}. In this study, the absolute dose threshold defining this surface was 4500 cGy. Again, this parameter

(ETV) was normalized to the V_{TB} and is therefore expressed as a percentage.

As previously mentioned, the fulfillment of institutional planning objectives for standard normal tissue structures was assessed (Table 2). To quantitatively compare the performance of VMAT plans with 3D plans in terms of their fulfillment of these criteria, for each plan type, mean values corresponding to each objective were computed. A statistical comparison of these means was performed for 3D and VMAT plans.

Finally, to evaluate and compare back and shoulder dosimetry between 3D and VMAT plans, volumes of the back and shoulder encompassed by isodose surfaces corresponding to dose threshold of 2000, 4500, 5000, and 5500 cGy were computed for each plan. These volumes are denoted as V₂₀₀₀^{Back}, V₄₅₀₀^{Back}, V₅₀₀₀^{Back}, V₅₅₀₀^{Back} and V₂₀₀₀^{Shoulder}, V₄₅₀₀^{Shoulder}, V₅₀₀₀^{Shoulder}, V₅₅₀₀^{Shoulder}, respectively. They were normalized to each structure's total volume and expressed as a percentage.

For each metric of this study, statistical significance of differences in mean values obtained for 3D and VMAT plans was tested using a paired, 2-tailed Student *t* test.

Results

The distributions of CTV₄₉₀₀^{Target} values for 3D and VMAT plans are shown in Fig. 1 which illustrates a narrow domain, centered around 98%, for VMAT plans (mean, 98.9%; ±1 SD: ±0.6%). In contrast, the 3D plan domain is broad and includes values as low as 90% reflecting insufficient CTV^{Target} dose delivery (mean, 95.4%; ±1 SD: ±2.4%). Clearly, coverage of CTV^{Target} by VMAT plans (*P* < .01) is superior.

The distributions of CTV_{HS}^{Target} values for 3D and VMAT plans are shown in Fig. 2 which illustrates a narrow domain clustered close to the prescription dose of 5000 cGy for VMAT plans (mean, 5449 cGy; SD, 88 cGy).

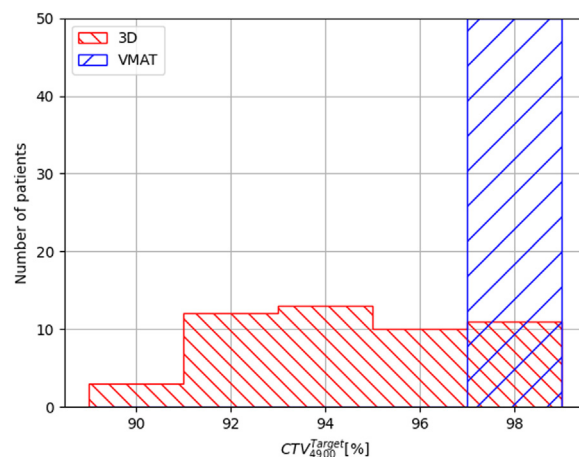


Figure 1 Histogram of CTV₄₉₀₀^{Target} for volumetric modulated arc therapy and 3-dimensional plans.

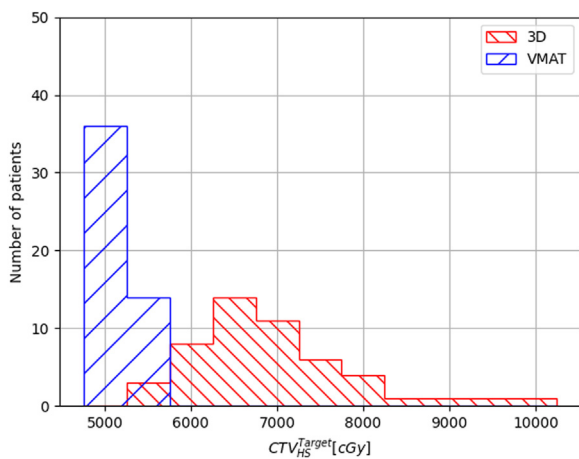


Figure 2 Histogram of CTV_{HS}^{Target} for both volumetric modulated arc therapy and 3-dimensional plans.

By comparison, the 3D plan domain is broader and extends to values as high as 10,000 cGy, reflecting significantly greater doses within CTV_{HS}^{Target} by 3D plans (mean, 7200 cGy; SD, 907 cGy). Hotspot doses this high were present on some 3D plans of this study because the nodal fields were prescribed to a percentage of the prescription isodose to minimize the size of the cold spot present at the match line. An example is shown in Fig. 3a. This demonstrates the presence of very high hotspots (blue isodose line in Fig. 3a is 10,000 cGy) of a 3D plan normalized in this manner. The corresponding VMAT plan isodoses shown in Fig. 3b reflect a more homogeneous dose. Clearly, dose uniformity within CTV_{HS}^{Target} for VMAT plans was superior ($P < .01$).

The distributions of V_{5000}^{Body} and V_{5500}^{Body} for 3D and VMAT plans are shown in Fig. 4a, b, respectively. The

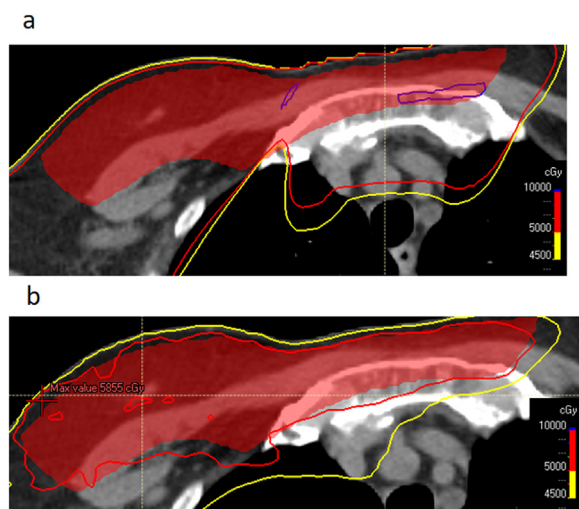


Figure 3 Three-dimensional (3D) plan target volume coverage and hotspots of 3D and volumetric modulated arc therapy plans. (a) shows the cold spot at the tangent field and IMC field junction of a 3D plan. (b) shows improved dose uniformity and target coverage in this region.

mean V_{5000}^{Body} for 3D plans was 56% greater than that found for VMAT plans. At 5500 cGy (110% of prescription), it was 1400% greater, reflecting the superior dose uniformity of VMAT plans. No doses > 5750 cGy present on VMAT plans. However, substantial volumes encompassed by doses as high as 130% of the prescription dose were present on 3D plans. These data clearly demonstrate global dose uniformity within V_{TB} (mean values of V_{5000}^{Body} , V_{5250}^{Body} , V_{5500}^{Body} , V_{5750}^{Body} , V_{6000}^{Body} , V_{6250}^{Body} , and V_{6500}^{Body} were all statistically lower in VMAT plans ($P < .01$).

Figure 5 shows the distribution of ETV found for 3D and VMAT plans. The mean ETV (± 1 SD) for 3D plans was more than double the value computed for VMAT plans (ie, 5.3% [$\pm 1.3\%$] vs 2.7% [$\pm 0.5\%$] for VMAT plans [$P < .01$]), reflecting a much greater volume of normal tissue receiving substantial dose in 3D plans versus VMAT plans.

Statistically significant ($P < .01$) smaller volumes were found within the shoulder for VMAT plans at all isodose levels in the 2000- to 5500-cGy range. Within the back, statistically significant ($P < .01$) smaller isodose surface volumes were observed for dose thresholds at or above 4500 cGy. While the mean value for V_{2000}^{Back} was slightly lower for 3D plans (26% vs 32% for VMAT plans), this difference is not clinically significant.

Table 2 contains mean values (± 1 SD) for 3D and VMAT plans corresponding to institutional treatment planning goals. Statistically significant differences in dose 13 of 17 planning objectives were observed between VMAT and 3D plans.

Discussion

This study quantitatively compared VMAT with 3D planning for breast cancer patients requiring breast/chest wall radiation therapy with CRNI using metrics that assess target volume dose homogeneity, plan dose homogeneity, target volume dose conformity, and standard normal tissue dose limits. Additionally, back and shoulder dose statistics were studied. Superior CTV_{HS}^{Target} dose coverage, dose uniformity, and dose conformity were observed in VMAT plans. VMAT plans also had fewer hotspots. VMAT plans had comparable or (usually) lower shoulder and posterior trunk (back) volumes defined by several dose thresholds. For the latter, significantly less volume received 2000 cGy with the VMAT plans. Other normal tissues also had reduced doses among VMAT plans. The mean ipsilateral lung V_{20} of 47.9% found for the 3D plans exceeds dose-volume histogram constraints used on national protocols for breast treatments, which is likely 1 of the reasons the patient was treated with VMAT. Our study found that the only normal tissue dose metrics that were slightly better among 3D plans when compared to VMAT plans were the mean contralateral breast/chest wall dose, mean and maximum celiac plexus/

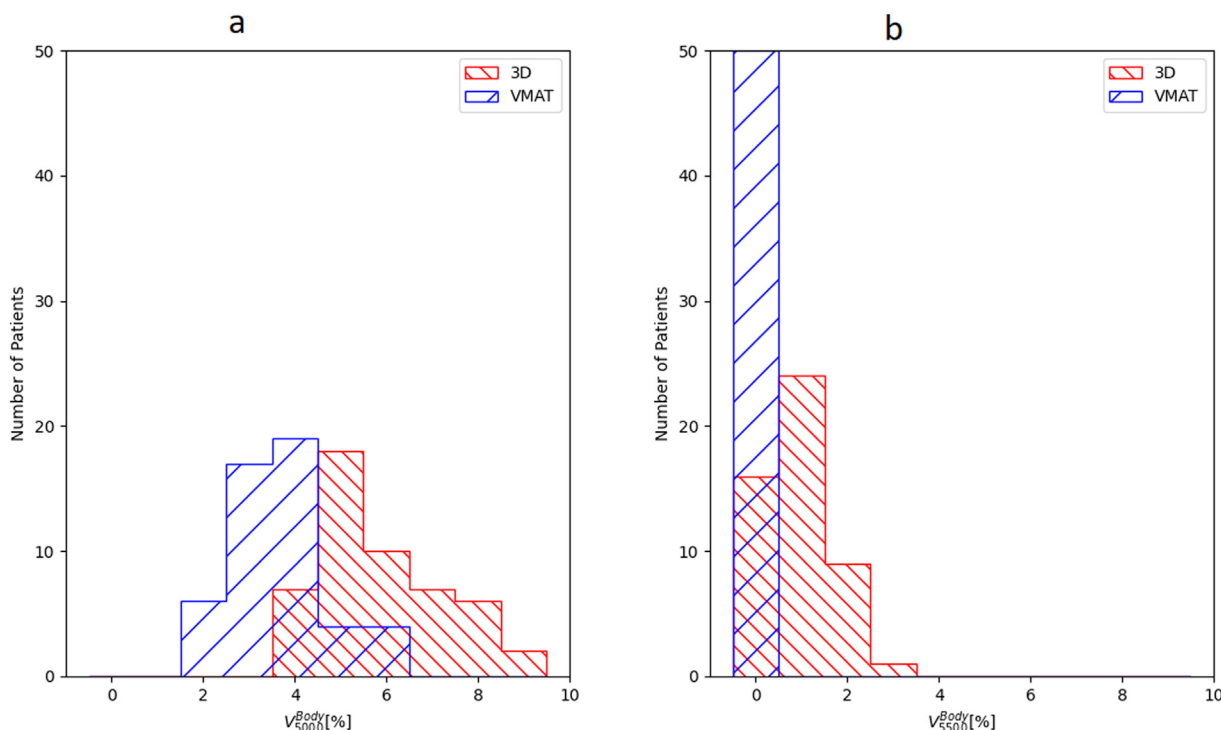


Figure 4 Histograms of body volumes receiving doses of 100% and 110% of the prescription dose (5000 cGy and 5500 cGy). (a,b) reflect improved dose conformity of VMAT plans in that the volumes receiving the prescription dose or higher are larger among 3D plans.

GE junction dose, mean liver mean dose, and mean stomach mean dose. However, this is to be anticipated due to the nature of VMAT planning in which a small dose is delivered to a larger volume of tissue as a compromise needed to deliver higher therapeutic doses to smaller volumes in a pattern that is more conformal to target volumes.

The potential for VMAT to improve target dose uniformity has been well established.^{12,14,34} Dose uniformity has also been related to improved outcomes as mentioned

earlier in the study by Donovan et al.¹⁴ In a randomized, phase 2 clinical trial for patients receiving radiation therapy to the breast and internal mammary chain, Ranger et al¹² also found that, compared to wide tangent field plans, VMAT improved nodal coverage. The Alliance A011202 protocol specifies several criteria for dose uniformity within target volumes.³⁴ It stipulates that < 10 cm³ of the “PTV Eval” is to receive no more than 115% of the prescription dose of 5000 cGy. However, it specifies an acceptable variation of up to 130% of the prescription dose. To try to cover 98% of CTV^{Target} with 98% of the prescribed dose, our 3D plans had a mean of 144% hot spots, yet only achieved 95.4% mean CTV coverage with 4900 cGy.

Radiation therapy planning often focuses on target coverage and dose to normal tissues. Nationally published standards³⁵ do not consider dose to the musculoskeletal regions such as the posterior trunk and the shoulder. We know from clinical experience and published data that radiation-induced fibrosis is correlated with total dose, fraction dose, and volume of tissue treated.³⁶ Minimizing exposure of posterior trunk soft tissues and the shoulder to radiation can limit the incidence and severity of fibrosis. This both facilitates and simplifies the potential use of the posterior trunk tissues for future reconstruction, particularly in thin patients who may be more dependent on this region for subsequent reconstruction. Additionally, patients are routinely counseled on the need for lifelong

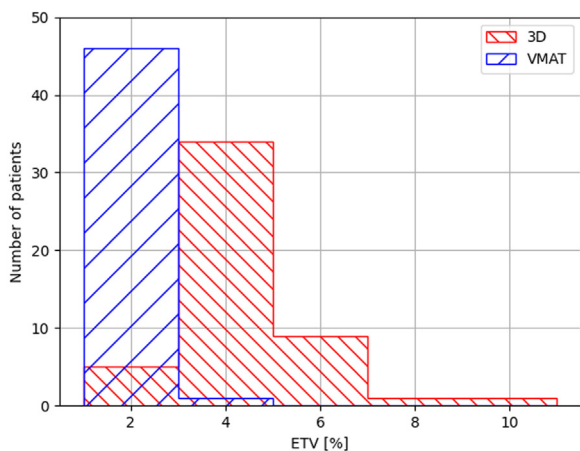


Figure 5 Histogram of ETV metric for both volumetric modulated arc therapy and 3-dimensional plans.

daily range of motion exercise of the arm and shoulder to minimize the effects of fibrosis of the shoulder girdle limiting range of motion, causing pain, and affecting activities of daily living. Often, physical therapy is necessary to help maintain full function. The less volume of back and shoulder musculature treated to doses above 4500 cGy would be expected to lessen the long-term effects of radiation on the function of the arm and shoulder. Bazan et al²⁶ evaluated the impact of intensity modulated radiation therapy to the shoulder dose. In patients receiving regional nodal irradiation, the QuickDASH²⁷ instrument was used to evaluate shoulder dose in a study of 410 patients. They found that in a subset of these patients, lower QuickDASH scores were observed following intensity modulated radiation therapy when compared to plans delivered using a 3D technique. Our study demonstrated a reduction in dose of 2000 cGy or more to the shoulder and 4500 cGy or more to the back. This reduction in dose is expected to reduce the risk of fibrosis of the shoulder and back musculature.

Questions on secondary cancer risk associated with VMAT treatments have been raised because at the low dose levels, there is an increased volume of normal tissue receiving a dose when compared to 3D treatments. However, in a study by Fogliata et al,³⁷ it was found that when treating the whole breast, VMAT may have the same risk of second cancer induction as 3D radiation therapy for contralateral OARs and may even lower acute and late normal tissue complication probabilities for ipsilateral OARs. They concluded that VMAT might be considered a safe technique for breast cancer treatment for those aspects. It must be pointed out that our 3D plans in fact did have excess volume of nontarget tissue treated to 4500 cGy or greater than our VMAT plans, and in fact the low dose to the ipsilateral lung as defined as volume receiving 1000 cGy or more (ipsilateral lung V_{10}) was higher in our 3D plans as well. Therefore, it becomes less clear which plan may be safer in terms of risk of secondary malignancy related to radiation.

VMAT offers not just dosimetric benefits, but also greater efficiency of planning and delivery. An important consequence is a reduction in patient wait times for patients before and during their treatment course. The time required during each treatment session is significantly lower with VMAT, particularly when compared with multifield setups required by 3D plans. This is not due to setup simplicity. Three-dimensional plans invariably require multiple isocenters. This adds extra setup time as patients are aligned patients to various isocenter locations.

Conclusions

Despite data in support of dosimetric advantages of VMAT for breast cancer patients requiring CRNI, comparative 3D plans are required for reimbursement

authorization by many healthcare insurance policies. Unless heart or lung doses exceed national guidelines with the 3D plan, some insurers may still not approve VMAT reimbursement even though a simple anatomic review can predict how problematic 3D planning would be. Questions regarding the impact of such requisites on overall treatment outcomes are also valid.

Congruent with prior studies, our study of 50 breast cancer patients requiring CRNI illustrates that VMAT provides a dosimetrically superior therapy as compared to 3D techniques. Although prior studies evaluated VMAT in specific clinical scenarios, eg, patients with left-sided disease only and/or smaller populations, this study strengthens support for the superiority of VMAT independent of disease laterality, particularly for those requiring more complicated external beam planning. It is a reasonable conclusion therefore that VMAT should be covered by insurance plans as a standard planning option for such patients. Why should they be denied this?

Disclosures

None.

Acknowledgments

Robin Kendall and David Swanson performed the statistical analysis.

References

1. Teoh M, Clark CH, Wood K, Whitaker S, Nisbet A. Volumetric modulated arc therapy: A review of current literature and clinical use in practice. *Br J Radiol*. 2011;84:967-996.
2. Hunte SO, Clark CH, Zyuzikov N, Nisbet A. Volumetric modulated arc therapy (VMAT): A review of clinical outcomes—what is the clinical evidence for the most effective implementation? *Br J Radiol*. 2022;95:20201289.
3. Racka I, Majewska K, Winiecki J. Three-dimensional conformal radiotherapy (3D-CRT) vs. volumetric modulated arc therapy (VMAT) in deep inspiration breath-hold (DIBH) technique in left-sided breast cancer patients—comparative analysis of dose distribution and estimation of projected secondary cancer risk. *Strahlenther Onkol*. 2023;199:90-101.
4. Sakka M, Kunzelmann L, Metzger M, Grabenbauer GG. Cardiac dose-sparing effects of deep-inspiration breath-hold in left breast irradiation: Is IMRT more beneficial than VMAT? *Strahlenther Onkol*. 2017;193:800-811.
5. Stanton C, Bell LJ, Le A, et al. Comprehensive nodal breast VMAT: Solving the low-dose wash dilemma using an iterative knowledge-based radiotherapy planning solution. *J Med Radiat Sci*. 2022;69:85-97.
6. Karpf D, Sakka M, Metzger M, Grabenbauer GG. Left breast irradiation with tangential intensity modulated radiotherapy (t-IMRT) versus tangential volumetric modulated arc therapy (t-VMAT): Trade-offs between secondary cancer induction risk and optimal target coverage. *Radiat Oncol*. 2019;14:156.

7. Zhang Y, Huang Y, Ding S, et al. A dosimetric and radiobiological evaluation of VMAT following mastectomy for patients with left-sided breast cancer. *Radiat Oncol*. 2021;16:171.
8. Zhang Z, Li D, Peng F, et al. Evaluation of hybrid VMAT advantages and robustness considering setup errors using surface guided dose accumulation for internal lymph mammary nodes irradiation of postmastectomy radiotherapy. *Front Oncol*. 2022;12:907181.
9. Sudha SP, Seenisamy R, Bharadhwaj K. Comparison of dosimetric parameters of volumetric modulated arc therapy and three-dimensional conformal radiotherapy in postmastectomy patients with carcinoma breast. *J Cancer Res Ther*. 2018;14:1005-1009.
10. Haertl PM, Pohl F, Weidner K, Groeger C, Koelbl O, Dobler B. Treatment of left sided breast cancer for a patient with funnel chest: Volumetric-modulated arc therapy vs. 3D-CRT and intensity-modulated radiotherapy. *Med Dosim*. 2013;38:1-4.
11. Pham TT, Ward R, Latty D, et al. Left-sided breast cancer loco-regional radiotherapy with deep inspiration breath-hold: Does volumetric-modulated arc radiotherapy reduce heart dose further compared with tangential intensity-modulated radiotherapy? *J Med Imaging Radiat Oncol*. 2016;60:545-553.
12. Ranger A, Dunlop A, Hansen VN, et al. A randomised phase II clinical trial comparing the deliverability and acute toxicity of wide tangent versus volumetric modulated arc therapy to the breast and internal mammary chain. *Clin Oncol*. 2022;34:526-533.
13. Murakami Y, Murakami Y, Kamima T, et al. Dosimetric comparison between three-dimensional conformal radiotherapy followed by electron beam boost and volumetric modulated arc therapy using concomitant boost for the heart and cardiac segments in patients with left-sided breast cancer at risk for radiation-induced cardiac toxicity. *Phys Med*. 2022;95:126-132.
14. Donovan E, Bleakley N, Denholm E, et al. Randomised trial of standard 2D radiotherapy (RT) versus intensity modulated radiotherapy (IMRT) in patients prescribed breast radiotherapy. *Radiother Oncol*. 2007;82:254-264.
15. Kaidar-Person O, Fortpied C, Hol S, et al. The association of internal mammary and medial supraclavicular lymph node radiation technique with clinical outcomes: Results from the EORTC 22922/10925 randomised trial. *Radiother Oncol*. 2022;172:99-110.
16. Blichert-Toft M, Rose C, Andersen JA, et al. Danish randomized trial comparing breast conservation therapy with mastectomy: Six years of life-table analysis. Danish Breast Cancer Cooperative Group. *J Natl Cancer Inst Monogr*. 1992:19-25.
17. National Comprehensive Cancer Network. Accessed July 1, 2023. https://www.nccn.org/professionals/physician_gls/pdf/breast.pdf.
18. Whelan TJ, Olivetto IA, Parulekar WR, et al. Regional nodal irradiation in early-stage breast cancer. *N Engl J Med*. 2015;373:307-316.
19. Stierman B, Afful J, Carroll MD, Margaret D, et al. National Health and Nutrition Examination Survey 2017–March 2020 Prepandemic Data Files—Development of Files and Prevalence Estimates for Selected Health Outcomes. National Center for Health Statistics; 2021. Accessed July 1, 2023; <https://www.ncbi.nlm.nih.gov/books/NBK606854/>.
20. Albornoz CR, Bach PB, Mehrara BJ, et al. A paradigm shift in U.S. Breast reconstruction: Increasing implant rates. *Plast Reconstr Surg*. 2013;131:15-23.
21. American Society of Plastic Surgeons. Plastic surgery statistics report. Accessed July 1, 2023. <https://www.plasticsurgery.org/documents/News/Statistics/2020/plastic-surgery-statistics-full-report-2020.pdf>.
22. Bellini E, Pesce M, Santi P, Raposio E. Two-stage tissue-expander breast reconstruction: A focus on the surgical technique. *BioMed Res Int*. 2017;2017:1791546.
23. Spear SL, Mesbahi AN. Implant-based reconstruction. *Clin Plast Surg*. 2007;34:63-73.
24. Kronowitz SJ, Hunt KK, Kuerer HM, et al. Delayed-immediate breast reconstruction. *Plast Reconstr Surg*. 2004;113:1617-1628.
25. Verma V, Ludmir EB, Mesko SM, et al. Commercial insurance coverage of advanced radiation therapy techniques compared with American Society for Radiation Oncology model policies. *Pract Radiat Oncol*. 2020;10:324-329.
26. Bazan JG, DiCostanzo D, Hock K, et al. Analysis of radiation dose to the shoulder by treatment technique and correlation with patient reported outcomes in patients receiving regional nodal irradiation. *Front Oncol*. 2021;11:617926.
27. Kennedy CA, Beaton DE, Smith P, et al. Measurement properties of the QuickDASH (Disabilities of the Arm, Shoulder and Hand) outcome measure and cross-cultural adaptations of the QuickDASH: a systematic review. *Qual Life Res*. 2013;22(9):2509-2547. <https://doi.org/10.1007/s11136-013-0362-4>.
28. NRG Oncology. RADCOMP Breast Atlas. Accessed July 1, 2023. <https://www.nrgoncology.org/About-Us/Center-for-Innovation-in-Radiation-Oncology/Breast-Cancer/RADCOMP-Breast-Atlas>.
29. Marks LB, Hebert ME, Bentel G, Spencer DP, Sherouse GW, Prosnitz LR. To treat or not to treat the internal mammary nodes: A possible compromise. *Int J Radiat Oncol*. 1994;29:903-909.
30. Arbab M, Frame R, Alluri P, et al. Master breast radiation planning: Simple guide for radiation oncology residents. *Adv Radiat Oncol*. 2024;9:101476.
31. Borghero YO, Salehpour M, McNeese MD, et al. Multileaf field-in-field forward-planned intensity-modulated dose compensation for whole-breast irradiation is associated with reduced contralateral breast dose: a phantom model comparison. *Radiother Oncol*. 2007;82:324-328.
32. Neal AJ, Torr M, Helyer S, Yarnold JR. Correlation of breast dose heterogeneity with breast size using 3D CT planning and dose-volume histograms. *Radiother Oncol*. 1995;34:210-218.
33. Gustafson NR, Burrier T, Butler B, Hunzeker A, Lenards N, Culp L. Correlation of hot spot to breast separation in patients treated with postlumpectomy tangent 3D-CRT using field-in-field technique and mixed photon energies. *Med Dosim*. 2020;45:134-139.
34. Alliance for Clinical Trials in Oncology. Alliance A011202: A randomized phase III trial comparing axillary lymph node dissection to axillary radiation in breast cancer patients (cT1-3 N1) who have positive sentinel lymph node disease after receiving neoadjuvant chemotherapy. Accessed July 1, 2023. <https://www.allianceforclinicaltrials.inoncology.org/main/cmsfile?cmsPath=/Public/Annual%20Meeting/files/A011202-Bouhey-May2019.pdf>.
35. Puckett LL, Kodali D, Solanki AA, et al. Consensus quality measures and dose constraints for breast cancer from the Veterans Affairs Radiation Oncology Quality Surveillance Program and American Society for Radiation Oncology expert panel. *Pract Radiat Oncol*. 2023;13:217-230.
36. Straub JM, New J, Hamilton CD, Lominska C, Shnayder Y, Thomas SM. Radiation-induced fibrosis: mechanisms and implications for therapy. *J Cancer Res Clin Oncol*. 2015;141:1985-1994.
37. Fogliata A, De Rose F, Franceschini D, et al. Critical appraisal of the risk of secondary cancer induction from breast radiation therapy with volumetric modulated arc therapy relative to 3D conformal therapy. *Int J Radiat Oncol*. 2018;100:785-793.